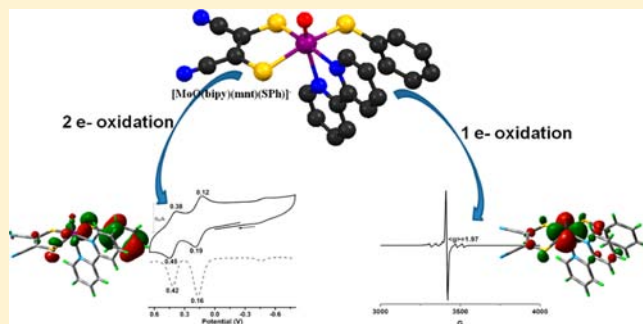


## Oxo–Mo(IV)(dithiolene)thiolato Complexes: Analogue of Reduced Sulfite Oxidase

Joyee Mitra<sup>†</sup> and Sabyasachi Sarkar<sup>\*,‡</sup><sup>†</sup>Department of Chemistry, Indian Institute of Technology Kanpur, Kanpur 208016, Uttar Pradesh, India<sup>‡</sup>Department of Chemistry, Bengal Engineering and Science University Shibpur, Howrah 711 103, West Bengal, India

## Supporting Information

**ABSTRACT:** A series of  $[\text{Mo}^{\text{IV}}\text{O}(\text{mnt})(\text{SR})(\text{N}-\text{N})]^-$  (mnt = maleonitriledithiolate; R = Ph, nap, *p*-Cl-Ph, *p*-CO<sub>2</sub>H-Ph, and *p*-NO<sub>2</sub>-Ph; N–N = 2,2'-bipyridine (bipy) and 1,10-phenanthroline (phen)) complexes analogous to the reduced active site of enzymes of the sulfite oxidase family has been synthesized and their participation in electron transfer reactions studied. Equatorial thiolate and dithiolene ligations have been used to closely simulate the three sulfur coordinations present in the native molybdenum active site. These synthetic analogues have been shown to participate in electron transfer via a pentavalent EPR-active Mo(V) intermediate with minimal structural change as observed electrochemically by reversible oxidative responses. The role of the redox-active dithiolene ligand as an electron transfer gate between external oxidants and the molybdenum center could be envisaged in one of the analogue systems where the initial transient EPR signal with  $\langle g \rangle = 2.008$  is replaced by the appearance of a typical Mo(V)-centered EPR ( $\langle g \rangle = 1.976$ ) signal. The appearance of such a ligand-based transient radical at the initial stage has been supported by the ligand-centered frontier orbital from DFT calculation. A stepwise rationale has been provided by computational study to show that the coupled effects of the diimine bite angle and the thiolato dihedral angle determine the metal- or ligand-based frontier orbital occupancy. DFT calculation has further supported the similarity between the reduced, semireduced, and oxidized resting state of the molybdenum center in Moco of SO with the synthesized complexes and their corresponding one-electron and fully oxidized species.



## INTRODUCTION

Sulfite oxidase (SO), a pyranopterin molybdenum oxo-transferase, participates in the physiologically critical oxidation of sulfite to sulfate, the terminal step in the degradation of sulfur-containing amino acids cysteine and methionine.<sup>1</sup> The molybdenum site in SO is reduced to Mo(IV) from Mo(VI) concomitant to the oxo-transfer reaction. The reduced  $\{\text{O}=\text{Mo}^{\text{IV}}\}$  center thus formed gets oxidized by two sequential steps of one-electron transfer via participation of oxidized cytochrome *b*<sub>5</sub>, generating an EPR-active  $\{\text{O}=\text{Mo}^{\text{V}}(\text{OH})\}$  intermediate.<sup>2</sup> *YedY*, a new member of the SO family isolated from *E. coli*, has been characterized in the Mo(V) state and is presumed to shuttle between Mo(IV) and Mo(V) oxidation states.<sup>3</sup> The structure of chicken liver SO (cSO) was solved in the product-bound reduced Mo(IV) state of the enzyme.<sup>4</sup>

The structure–function relationship is helpful in assessing the reaction mechanism of an enzyme. On the basis of the structure of the molybdenum active site of cSO, i.e., a pyranopterindithiolene ligand coordinated to the oxo–molybdenum center along with a cysteine residue from the apoprotein, the minimum structural model to mimic the active site requires a dithiolene coordination to oxo–Mo center along with thiolate ligation. The square pyramidal geometry around molybdenum in the native active site remains stabilized as it is

encased in the protein fold that thwarts approach of unwanted water, thereby reducing the possibility of hydrolysis and dimerization, though a dimeric Mo(V) species is thermodynamically more stable compared to a monomeric Mo(V). In comparison to reports of forward oxo-transfer reaction,<sup>5</sup> regeneration of the molybdenum active site on electron transfer from Mo(IV) via Mo(V) intermediate has largely been neglected. Few synthesized complexes possess the essential dithiolene ligation to serve as analogues to the semireduced SO-like  $[\text{Et}_4\text{N}][\text{MoOCl}_2(\text{S}_2\text{C}_2\text{Me}_2)]$  and  $[\text{Et}_4\text{N}][\text{MoOCl}_2(\text{bdt})]$ .<sup>6</sup> These show Mo(V) rhombic EPR signal and can be electrochemically reduced to Mo(IV), though the reduced complexes were not isolated. Some nondithiolene oxo–Mo(V) complexes were reported with a view to understand the EPR signature of SO.<sup>7–9</sup> Coordination of three sulfur atoms in the equatorial plane (two of which are from dithiolene) is the essential qualification for a compound to be considered as a structural analogue of reduced sulfite oxidase. No synthetic complex mimicking the fully reduced state of sulfite oxidase has been synthesized with dithiolene and thiolato ligation to date.

Received: November 14, 2012

Published: March 6, 2013

The chemistry of molybdenum dithiolenes has been dominated by the study of bis(dithiolene) complexes on account of a dithiolene linkage in the molybdenum cofactor<sup>2,10</sup> and also tris(dithiolene) complexes.<sup>11</sup> Mo(VI) complexes were stabilized especially with dioxo coordination for modeling the molybdenum site in SO.<sup>5</sup> Attachment of only one dithiolene and one thiolate ligand to Mo(VI) instead of bis- or tris-dithiolene coordination would impose instability in such a compound and thus render the system very reactive. The isolated cofactor in the reduced state of SO<sup>4</sup> has a spectator oxo group along with one ene-dithiolene ligation, cysteinyl sulfur, and a hydroxo/water molecule to satisfy a pentacoordinated active site. Our approach is to synthesize some complexes with similar coordination using maleonitriledithiolate (mnt) to proxy the pyranopterindithiolate and benzenethiolate as a substitute for cysteinyl coordination. We employed aromatic diimines to block the fifth and sixth coordination sites, thereby thwarting hydrolysis and dimerization of the synthesized complexes even in the presence of traces of moisture. In this synthetic approach the ligand arrangement forms tetravalent mononuclear hexacoordinate molybdenum complexes, [Mo<sup>IV</sup>O(mnt)(SR)(N–N)]<sup>–</sup> (mnt = maleonitriledithiolate; SR = unsubstituted and para-substituted benzene thiolates; N–N = 2,2'-bipyridine (bipy) and 1,10-phenanthroline (phen) designated as **a** and **b** in the text). It is worth noting that oxygen or nitrogen as the donor atom has been proposed to occupy the sixth coordination site around molybdenum in YedY.<sup>3b</sup>

## EXPERIMENTAL SECTION

All reactions and manipulations were performed under an argon atmosphere using a modified Schlenk technique. *p*-Nitrothiophenol, *p*-chlorothiophenol, 4-mercaptobenzoic acid, and thionaphthol were purchased from Sigma Aldrich Ltd. All other chemicals were purchased from S. D. Fine Chemicals Ltd., India, and used without further purification. Solvents were dried and distilled according to standard procedures. [NBu<sup>n</sup>]<sub>2</sub>[Mo<sub>2</sub>O<sub>4</sub>(mnt)<sub>2</sub>]<sup>12</sup> was prepared according to the literature reported procedure.

**Physical Methods.** Electronic absorption spectroscopic measurements were performed using a Perkin-Elmer Lambda35 UV–vis spectrophotometer. Infrared spectra were recorded on a Bruker Vertex 70 FT-IR spectrophotometer. The sample was mixed with KBr and pressed as disks. To obtain a good signal-to-noise ratio, 32 scans were recorded. Elemental analyses for carbon, hydrogen, and nitrogen were performed with a Perkin-Elmer 2400 microanalyzer. Cyclic voltammetric measurements were carried out with BASi Epsilon–EC Bioanalytical Systems, Inc. Cyclic voltammograms of 10<sup>–3</sup> M solution of all complexes in dichloromethane were recorded using a glassy carbon electrode as the working electrode with 0.2 M Bu<sup>n</sup><sub>4</sub>PF<sub>6</sub> as the supporting electrolyte, Ag/AgCl electrode as the reference electrode, and platinum wire as the auxiliary electrode. All electrochemical measurements were performed under argon at 298 K. Potentials were referenced against ferrocene (Fc) and are reported relative to E<sub>1/2</sub>(Fc<sup>+</sup>/Fc) = 0.459 V vs Ag/AgCl electrode. Electron paramagnetic resonance spectra were recorded on a Bruker Biospin EMX EPR X-Band Spectrometer with a frequency of 9.856 GHz, microwave power of 0.2 mW, modulation amplitude of 5 G, and time constant of 10 ms at room temperature and also at 120 K using liquid nitrogen as the coolant. EPR parameters were calculated using Bruker WINEPR SimFonia. ESI mass spectra were measured on Waters Micromass Q TOF Premier Mass Spectrometer. Samples (dissolved in DCM) were introduced into the ESI source through a syringe pump at a rate of 5 μL per min. The ESI capillary was set at 3.5 kV, and the cone voltage was 10 V.

**X-ray Crystallography.** Suitable diffraction-quality crystals were obtained from the crystallization procedure described in each

synthesis. Diffraction data for all complexes were collected on a Bruker-AXS SMART APEX CCD diffractometer using Mo K $\alpha$  radiation  $\lambda = 0.71073$ . The crystal used for analysis was glued to a glass fiber and mounted on a BRUKER SMART APEX diffractometer. Cell constant was obtained from least-squares refinement of three-dimensional centroids through the use of CCD recording of narrow  $\omega$  rotation frames, completing almost all reciprocal space in the stated  $\theta$  range. All empirical absorption correction was applied using the SADABS program. Data was collected with SMART 5.628 (BRUKER, 2003) and integrated with the BRUKER SAINT<sup>13</sup> program. The temperature during data collection was maintained at 100 K for most of the crystals and 273 K for five of them. Structures were solved using SIR97<sup>14</sup> and refined using SHELXL97,<sup>15</sup> and thermal ellipsoid plots were generated using ORTEP-3<sup>16</sup> integrated within the WINGX suite of programs. The space groups of the compounds were determined on the basis of the lack of systematic absence and intensity statistics. Full matrix least-squares/difference Fourier cycles were performed which located the non-hydrogen atoms. All non-hydrogen atoms were refined with anisotropic displacement parameters. All complexes in the present study have one cation and one anion in their respective asymmetric unit except for the neutral dimeric complex **1** and monomeric **2a**, **3a**, and **3b**, which have two crystallographically independent units in their respective crystal lattice. Additional symmetry has been checked through PLATON. Of these two similar units, only one has been described with its ORTEP plot. The DCM molecule is present in the lattice of **1**, **2a**, **3a**, **4a**, **6a**, and **6b**. **2b** suffered from disorder of unidentified solvent (DCM/Petroleum ether) in the interstitial position, which was not included in the refinement but was removed using the SQUEEZE procedure from PLATON.

**EPR Measurements.** A few grains of I<sub>2</sub> (varied amount was used: substoichiometric, equivalent, and excess with respect to the complex) and Mo(IV) complexes were placed in the EPR tube and cooled using liquid nitrogen under inert atmosphere. A few drops of DCM (degassed) were added to the tube by raising the solid above liquid nitrogen, and once the DCM mixes with the solid it is frozen instantly. EPR spectra of such frozen solutions were recorded. After rapid recording of the EPR spectrum the sample was thawed under argon flow to room temperature and the EPR spectrum was recorded again. This solution was refrozen to check the stability of the EPR of the generated species with time. Spin quantitation was carried out to calculate the number of spins per gram (and subsequently the number of spins per molecule) of the samples using the stable radical 1,3-bisdiphenylene-2-phenylallyl (BDPA) (number of spins 1.6 × 10<sup>19</sup> g<sup>–1</sup>) as the standard.

**Computational Details.** DFT calculations were performed using the Gaussian 03 (Revision B.04)<sup>17</sup> package. Molecular orbitals were visualized using “Gauss View”. The method used was Becke’s three-parameter hybrid-exchange functional, the nonlocal correlation provided by the Lee, Yang, and Parr expression, and the Vosko, Wilk, and Nuair 1980 local correlation functional (III) (B3LYP).<sup>18</sup> The 6-31G\*+ basis set was used for C, N, Cl, S, O, and H. For another set of calculations, the BP86<sup>19</sup> functional was used instead of B3LYP. The LANL2DZ basis set<sup>20</sup> and LANL2 pseudopotentials of Hay and Wadt were used for the Mo atom.<sup>21</sup> Single-point calculations were done in both the gas phase and DCM using Klamt’s form of the conductor reaction field (COSMO)<sup>22</sup> solvent model. Molecular orbitals were analyzed using the AOMix program.<sup>23</sup> Initial geometries were taken from the crystal structures and used without further optimization. For the one- and two-electron-oxidized species after electron transfer, very little structural change was observed on optimization of the starting geometries. Time-dependent DFT calculations were also carried out using the same functional. For these calculations, singlet excited states were calculated based on the singlet ground state geometry. Forty lowest singlet excited states having oscillator strengths greater than 0.01 were considered for TDDFT calculations on incorporation of solvent dielectric. Dichloromethane (DCM) was the chosen solvent. Calculations derived from the reported crystal structure of cSO were used for comparison.

$[\text{Mo}_2\text{O}_3(\text{mnt})_2(\text{phen})_2]\cdot\text{CH}_2\text{Cl}_2$  (**1**). A 50 mg (0.05 mmol) amount of  $[\text{NBu}^n_4]_2[\text{Mo}_2\text{O}_4(\text{mnt})_2]^{12}$  was dissolved in 3 mL of dichloromethane. A 20 mg (0.1 mmol) amount of 1,10-phenanthroline was added into it. Dry HCl vapor was passed through it at 0 °C, when the solution acquired a violet color. On standing overnight, deep violet diffraction-quality crystals of **1** separated out. These were filtered, washed with petroleum ether, and vacuum dried. Yield: 50%. Analytical data for **1**:  $\text{C}_{32}\text{H}_{16}\text{Mo}_2\text{N}_8\text{O}_3\text{S}_4$ , MW 880.67. FTIR ( $\text{cm}^{-1}$ ):  $\nu_{\text{CN}}$  2208,  $\nu_{\text{Mo=O}}$  974,  $\nu_{\text{Mo-N}}$  847. Anal. Calcd for  $\text{C}_{32}\text{H}_{16}\text{Mo}_2\text{N}_8\text{O}_3\text{S}_4$ : C, 43.64; H, 1.83; N, 12.72. Found: C, 43.51; H, 1.78; N, 12.81.  $m/z = 881.77$ , corresponding to  $\text{C}_{32}\text{H}_{16}\text{Mo}_2\text{N}_8\text{O}_3\text{S}_4$ .

$[\text{NBu}^n_4][\text{MoO}(\text{mnt})(\text{SPh})(\text{bipy})]\cdot\text{CH}_2\text{Cl}_2$  (**2a**). A 50 mg (0.05 mmol) amount of  $[\text{NBu}^n_4]_2[\text{Mo}_2\text{O}_4(\text{mnt})_2]^{12}$  was dissolved in 3 mL of dichloromethane. A 16 mg (0.1 mmol) amount of 2,2'-bipyridine was added to it. A 6-fold excess of thiophenol was added into the mixture, which was stirred for 6 h. A blue solution was obtained along with precipitation of a purple-red-colored compound, which was separated by filtration. This was analyzed and matched with a previously reported complex  $[\text{NBu}^n_4]_2[\text{Mo}_2\text{O}_3(\text{mnt})_2(\text{SPh})_2]^{12}$ . A 10 mL amount of petroleum ether (60–80 °C) was layered over the blue filtrate and allowed to stand for 2 days at 4 °C to obtain dark blue-colored rectangular block-shaped diffraction-quality crystals. Analytical Data for **2a**:  $\text{C}_{36}\text{H}_{39}\text{MoN}_5\text{OS}_3$ , MW 749.87. FTIR ( $\text{cm}^{-1}$ ):  $\nu_{\text{CN}}$  2191,  $\nu_{\text{Mo=O}}$  921,  $\nu_{\text{Mo-N}}$  747. Anal. Calcd for  $\text{C}_{36}\text{H}_{39}\text{MoN}_5\text{OS}_3$ : C, 57.66; H, 5.24; N, 9.34. Found: C, 57.69; H, 5.15; N, 9.42.  $m/z = 517.48$ , anionic mass corresponding to  $\text{C}_{20}\text{H}_{13}\text{MoN}_4\text{OS}_3^-$ .

$[\text{NBu}^n_4][\text{MoO}(\text{mnt})(\text{SPh})(\text{phen})]$  (**2b**). A 50 mg (0.05 mmol) amount of  $[\text{NBu}^n_4]_2[\text{Mo}_2\text{O}_4(\text{mnt})_2]^{12}$  was dissolved in 3 mL of dichloromethane. A 20 mg (0.1 mmol) amount of 1,10-phenanthroline was added into it. To it a 6-fold excess of thiophenol was added and stirred for 4 h. A dark blue solution was obtained along with precipitation of a purple-red-colored compound. The precipitate on analysis was characterized as a previously reported complex  $[\text{NBu}^n_4]_2[\text{Mo}_2\text{O}_3(\text{mnt})_2(\text{SPh})_2]^{12}$ . An 8 mL amount of petroleum ether (60–80 °C) was layered over the blue filtrate and allowed to stand undisturbed at 4 °C to obtain dark blue-colored rectangular block-shaped diffraction-quality crystals within 2 days. These were filtered, washed with petrol ether, and dried under inert atmosphere. Yield: 55%. Analytical data for **2b**:  $\text{C}_{38}\text{H}_{39}\text{MoN}_5\text{OS}_3$ , MW 773.89. FTIR ( $\text{cm}^{-1}$ ):  $\nu_{\text{CN}}$  2192,  $\nu_{\text{Mo=O}}$  928,  $\nu_{\text{Mo-N}}$  839. Anal. Calcd for  $\text{C}_{38}\text{H}_{39}\text{MoN}_5\text{OS}_3$ : C, 58.98; H, 5.08; N, 9.05. Found: C, 58.89; H, 4.95; N, 9.11.  $m/z = 541.50$ , anionic mass corresponding to  $\text{C}_{22}\text{H}_{13}\text{MoN}_4\text{OS}_3^-$ .

**3a–6b** were synthesized following similar procedure using different thiols, details of which are provided as Supporting Information.

## RESULTS AND DISCUSSION

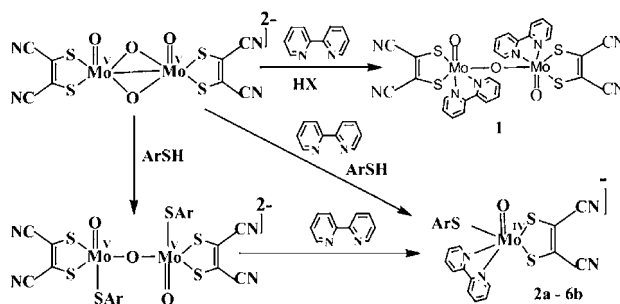
Formation of dimeric core  $\{\text{Mo}_2\text{O}_4\}$  is common in  $\text{Mo}^{\text{V}}$  chemistry, which is partially cleaved in acidic medium retaining one bridging oxo group to form a  $\{\text{Mo}_2\text{O}_3\}$  core.<sup>12</sup> The chemistry behind such a reaction could readily be interpreted by protonation of the bridging oxo to yield  $\text{Mo-OH}$ -like species, which resulted in cleavage of the oxo bridge. The conjugate base of the acid was found to be attached to the vacant fifth coordination position around the metal center.<sup>12</sup> In the presence of moisture, such a species is susceptible to hydrolysis to revert to the starting  $\{\text{Mo}_2\text{O}_4\}$  complex at room temperature via a pentacoordinated  $\text{Mo}(\text{V})$  monomeric  $\text{Mo-OH}$  species.<sup>12,24</sup> Similar reactivity was observed on treating  $[\text{Mo}_2\text{O}_4(\text{mnt})_2]^{2-}$  with benzenethiol; a  $\{\text{Mo}_2\text{O}_3\}$  complex coordinated to thiolate was obtained, i.e., each molybdenum center was coordinated to three equatorial sulfur atoms.<sup>12</sup> A variety of thiolate ligands were used to achieve a three sulfur-coordinated monomeric  $\text{Mo}(\text{V})\text{-OH}$  species, which could be an exact mimic of half-regenerated sulfite oxidase. Cleavage of the linear oxo bridge in the  $\{\text{Mo}_2\text{O}_3\}$  core is difficult due to extensive  $\pi$  delocalization supplementing the  $\sigma$  bond, leading to

a strong antiferromagnetic interaction.<sup>25</sup> The solution pH could not be lowered due to protonation of the coordinated mnt, resulting in its dissociation at  $\text{pH} < 5$ , forming the kelly green stable tris complex,  $[\text{Mo}(\text{mnt})_3]^{2-}$ . Strong organic acid like methanesulfonic acid forms a  $\text{Mo}(\text{V})$  sulfonato-bridged complex.<sup>12</sup> Thus, every attempt to synthesize  $\{\text{O}=\text{Mo}^{\text{V}}\text{-OH}\}$  species coordinated to three equatorial sulfur atoms was thwarted by the inherent drive for dimerization under the experimental condition. However, a  $\text{Mo}(\text{IV})$  monomeric species was thought to be isolable in the presence of a strong bidentate ligand under reducing environment (in the presence of thiol), which would prevent the dimerization reaction. Our quest for a suitable chelating agent was fulfilled by aromatic diimines (2,2'-bipyridine and 1,10-phenanthroline), which were known to coordinate effectively to molybdenum.<sup>26</sup>

Ten complexes of general formula  $[\text{Mo}^{\text{IV}}\text{O}(\text{mnt})(\text{SR})(\text{N-N})]^-$  were synthesized and characterized having three sulfur coordinations in the equatorial plane: two from the dithiolene moiety and a thiolate residue similar to the coordination environment around the molybdenum active site in SO. Of the two diimines used, bipy has two pyridine units joined by a single bond and thus can rotate freely to adjust its chelating ability in contrast to phen where the aromatic ring in between two pyridine halves made the molecule rigid. Such difference in these diimines may impose varied structural distortions in these compounds.

It has been observed that phen complexes are formed much faster compared to their bipy analogues. Phen being a rigid ligand can exist only in the syn configuration. Thus, binding to the metal center is facilitated. Bipy, on the other hand, is flexible due to single-bond rotation via the bipyridine axis, and both the syn and the anti rotamers exist. Effective coordination requires the presence of the syn isomer. These reactions also depend on the acidity of the thiols, the electron-withdrawing thiols being stronger acid, facilitating protonation of the starting oxo dimeric complex.<sup>27</sup>

**Structure Description.** The  $\text{Mo}(\text{V})$  dimeric complex coordinated to phen, **1**, and 9 out of 10 synthesized monomeric  $\text{Mo}(\text{IV})$  complexes (**2a–6b**, see Figure 1) were structurally characterized. Bond lengths and angles of **1** are in good agreement with the other reported  $\{\text{Mo}_2\text{O}_3\}$  dithiolene complexes.<sup>8b,12</sup> **1** exhibits a distorted octahedral geometry around each pentavalent molybdenum center; the apical position occupied by terminal oxo group is placed at a distance of 1.691 Å and the axial  $\text{Mo-N}$  at 2.324 Å. The basal plane is



Ar—Ph, **2a** and **2b**: nap, **3a** and **3b**: p-Cl-Ph, **4a** and **4b**: p-CO<sub>2</sub>H-Ph, **5a** and **5b**: p-NO<sub>2</sub>-Ph, **6a** and **6b** a denotes bipy and b denotes phen ligated complexes

**Figure 1.** Synthetic scheme for dimeric and monomeric molybdenum complexes **1–6b**. 1,10-Phenanthroline has been used instead of 2,2'-bipyridine for complexes **b**.

defined by two S donors from mnt, one nitrogen ligand from the diimine, and one bridging oxo. Mo atoms are located 0.33 Å above the basal plane. Terminal oxo groups coordinated to the two molybdenum centers are anti to each other. Linear oxo at 1.879 Å bridges the two units with a crystallographically imposed inversion center. Mo–S distances are 2.404 and 2.456 Å; the Mo–S bond trans to the bridging oxo is slightly elongated. The basal Mo–N bond distance of 2.237 Å is shorter than the apical Mo–N bond. C=C and C–S distances are 1.35 and 1.75 Å, respectively, which are sufficiently close to the typical bond lengths of C=C 1.331 Å and C–S 1.76 Å to establish the mnt ligand as a classical 1,2-dithiolene.<sup>5d,6,28,29</sup> The ORTEP plot of **1** is shown in Figure 2.

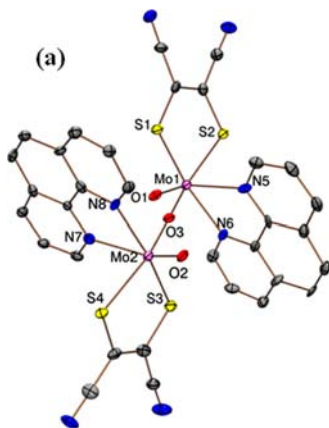


**Figure 2.** Perspective view of **1** depicted at 50% probability thermal ellipsoids. All H atoms have been omitted for clarity.

All structurally characterized monomeric complexes presented here are isostructural. These monoanionic complexes have a slightly distorted octahedral geometry around the molybdenum center. Deviation from ideal octahedral geometry results from the electronic repulsions between the out of plane p orbitals of the equatorial ligands and the  $\pi$  orbitals of the molybdenyl (Mo=O) unit. The basal plane is defined by two sulfur atoms from mnt, one thiolate residue and one nitrogen center from the diimine. The two apical positions are occupied by one terminal oxo group at an average distance of 1.69 Å and one nitrogen atom from the diimine at an average distance of 2.31 Å. The mean C=C and C–S distances are 1.35–1.38 and 1.74–1.76 Å, respectively. The diimine nitrogen atom anti to the molybdenyl group is bonded at a slightly longer distance ( $\sim 0.12$  Å) from the molybdenum center, which can be attributed to the influence of the apical oxo group. This distance increases slightly in phen complexes. Bipy (and phen) behaves as a neutral donor in all cases, as observed from the C<sub>1</sub>–C<sub>1</sub>' distance of 1.469 Å.<sup>30</sup> The Mo–S bonds of 2.43–2.45 Å are somewhat longer as compared to other oxo–Mo(IV) complexes though not unprecedented.<sup>31</sup> An average diimine bite angle of 69.8–71.1° and dithiolene bite angle of 84.3–84.9° are observed. The O–Mo–S–C torsion angle ranges from 93° to 105°, which is very close to the reported value of  $\sim 90^\circ$  for cSO.<sup>4</sup> This suggests that the steric factor does not play a significant role in the orientation of the thiolate residue. The change in the diimine does not significantly affect the geometry around Mo, though subtle changes in the bond angles and torsion angle are observed (Table S5, Supporting Information). The  $\pi$ – $\pi$  stacking of the aromatic moieties is observed in all complexes and more prominent for the phen complexes and

also in **3a** and **3b** due to the presence of thionaphthol. Complexes **5a** and **5b** exist as hydrogen-bonded dimer due to the *p*-carboxylate residues of the thiolate. ORTEP plots of the anions of **2a** and **2b** have been appended in Figure 3. The other

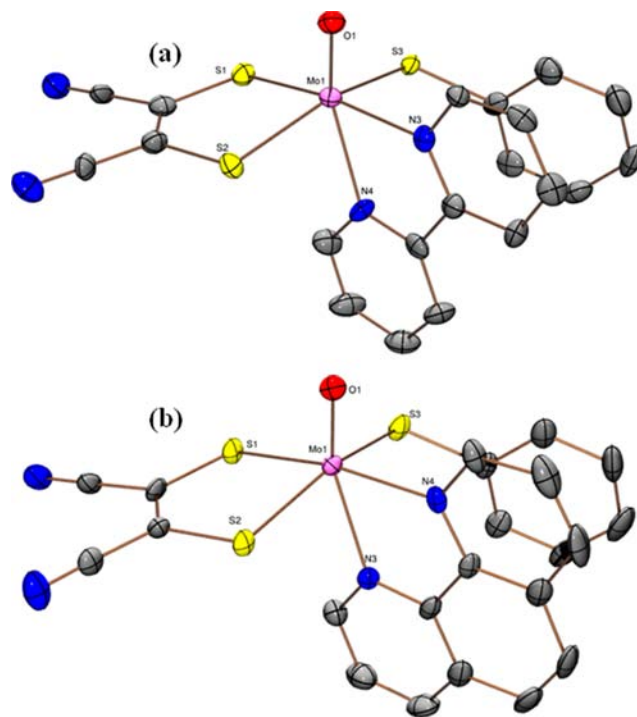


**Figure 3.** Perspective view of the anions of **2a** and **2b** depicted at 50% probability thermal ellipsoids. All H atoms have been omitted for clarity.

isostructural complexes are presented as Supporting Information (Figures S1 and S2). The increase in torsion angle of the thiolate moiety coupled with the diimine bite results in subtle changes in observed reactivity in **2a** and **2b**, and this has been discussed in subsequent sections. Important structural parameters for the synthesized complexes are collected in Tables S1–S3 (Supporting Information). Relevant bond lengths and angles have been tabulated in Tables S4 and S5 (Supporting Information).

**Spectroscopic Characterization.** The electronic spectrum of **1** in dichloromethane showed the signature of {Mo<sub>2</sub>O<sub>3</sub>} species<sup>12</sup> consisting of two absorption bands in the visible region: a broad band around 600 nm and a relatively high-intensity band at 498 nm. Electronic spectra of **2a–6b** reveal a low-energy metal-based transition in all complexes which is characteristic of M(diimine)(dithiolene) complexes.<sup>32</sup> **2a–6b** show a broad charge transfer transition in the low-energy region (580–620 nm) which is MLCT in nature. On photoexcitation, the electronic transition takes place from the filled metal-based HOMO to the vacant  $\pi^*$  LUMO of the diimine as supported by TDDFT calculations. Thus, the metal center is formally oxidized and the diimine is reduced, providing interesting examples for investigation of the electron transfer phenomenon. This MLCT state has a very short lifetime and is structurally similar to the ground state. It has been observed that the molar extinction coefficient of the broad MLCT transition in phen complexes is higher than that of their bipy analogues in the present case. This aspect has also been reflected in the TDDFT calculation of the complexes in DCM

solvent. The similar nature of this band in all complexes validates that there is no significant effect of the thiolate ligand. The slight shift of this low-energy MLCT band to higher energy is observed for thiolates bearing an electron-donating substituent. Two representative examples one each for bipy- and phen-substituted complexes have been presented in Figure 4a and 4c, respectively, with their corresponding TDDFT

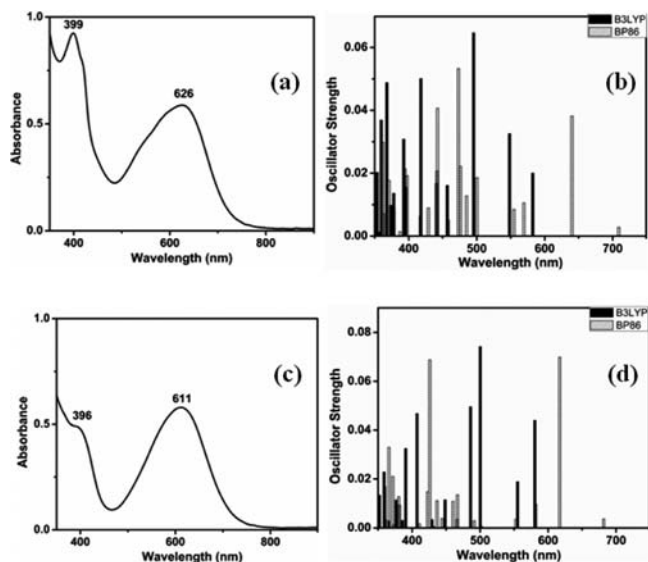


**Figure 4.** Electronic absorption spectra of (a) **2a** and (c) **2b** in DCM at  $10^{-4}$  M. Corresponding TDDFT assignments are provided in b and d using the B3LYP (black bar) and BP86 (gray bar) functionals, respectively.

assignments using the B3LYP and BP86 functional in Figure 4b and 4d, respectively. High-energy intense intraligand charge transfer transitions around 365–400 nm are also observed for each complex. High energy intraligand  $n-\pi^*$  and  $\pi-\pi^*$  electronic transitions can also be correlated from TDDFT which depict the involvement of ligand-centered orbitals in the higher energy electronic transitions. Both the B3LYP and the BP86 functional have been extensively used in describing  $M(\text{diimine})(\text{dithiolene})^{32,33}$  complexes. It is noted that a hybrid functional like B3LYP is more appropriate in describing these systems as compared to a pure functional like BP86 but not in all cases<sup>32,34,35</sup> as a higher amount of exact exchange in the functional favors high-spin states.<sup>34</sup> In the present case, it was observed that results with the BP86 functional are more in agreement with the experimentally observed MLCT transition at longer wavelength compared to B3LYP-derived results. However, not much difference is observed in the frontier orbital diagrams obtained with these two functionals.

An attempt has been made to compare the structure of the synthesized complexes with that of cSO and other members of the SO family. It is known that cSO was crystallized in its product-bound reduced state.<sup>4</sup> Understandably, the molybdenum active site in cSO<sup>4</sup> provides the best match for the synthesized complexes. *E. coli* oxidoreductase *YedY* also provides a good match apart from assimilatory nitrate reductase (Supporting Information Figure S3). The second oxygen moiety occupying the fifth coordination position in the active site of the native protein almost bisects the diimine bite angle of the synthesized complexes. In spite of the “dithiolene fold angle” effect,<sup>36</sup> which does not allow the match of the oxidized

and reduced (dithiolene)Mo–monooxo species, structural fitting of the dithiolene planes with the native active site in *YedY* provides a reasonable match.

**EPR Analysis.** **2a–6b** are in the Mo(IV) state with a terminal {Mo=O} moiety and hence EPR silent. These are chemically oxidized by one electron (vide supra) to display X-band EPR spectra at room temperature (also at 120 K). A typical molybdenum-based EPR spectrum consisting of one intense signal due to 75% <sup>96,98</sup>Mo ( $I = 0$ ) and six satellite lines due to 25% abundance of <sup>95,97</sup>Mo ( $I = 5/2$ ) is observed in solution. The isotropic  $\langle g \rangle = 1.976$  and  $\langle A \rangle = 42$  G are very similar to that observed for substrate-reduced SO.<sup>37</sup> The EPR spectrum of **2a** in solution at room temperature is presented in Figure 5a. Its frozen EPR spectrum at 120 K showed an almost

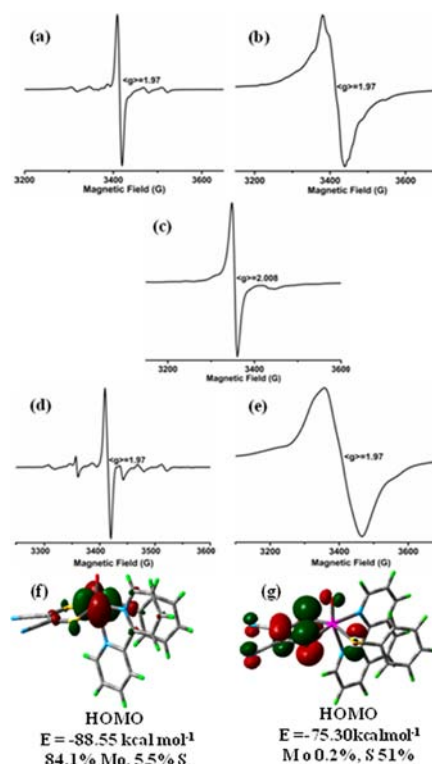


**Figure 5.** X-Band EPR spectra of one-electron-oxidized species of **2a** in DCM at (a) room temperature and (b) 120 K; (c) frozen solution EPR spectrum of **2b** characteristic of a transient radical species. On thawing this to solution the EPR spectrum (d) appears similar to a and on refreezing e is obtained similar to b. Corresponding SOMO of oxidized **2a** and **2b** are shown in f and g, respectively.

isotropic signal where satellites due to <sup>95,97</sup>Mo ( $I = 5/2$ ) are still visible in the relatively broad EPR signal as shown in Figure 5b. Complex **2b** which is the phen analogue of **2a** showed a different EPR spectrum to address the great topical interest. The one-electron-oxidized **2b** when immediately frozen in DCM matrix showed an EPR signal with  $\langle g \rangle = 2.008$  (Figure 5c), suggesting that the unpaired electron is ligand based and hence radical in nature. This frozen spectrum on thawing to room temperature changed with the appearance of characteristic six satellite resonances (Figure 5d) due to <sup>95,97</sup>Mo hyperfine splitting with an intense signal at its center with  $\langle g \rangle = 1.97$  similar to that shown in Figure 5a. However, on refreezing this thawed solution the original free-radical-type EPR signal was replaced by an almost isotropic signal (Figure 5e) with typical  $\langle g \rangle = 1.97$ . It may be presumed that on

chemical oxidation the ligand part gets oxidized first and such state of oxidation can be uniquely preserved under frozen DCM in **2b**. The radical during thawing of the frozen solution gained an electron from the Mo(IV) center, resulting in irreversible formation of Mo(V) species. Therefore, in the regeneration stage of the native active site a similar path of electron flow could be anticipated. In this study assignment of a metal-based or ligand-based unpaired electron is consistent with the composition of the singly occupied molecular orbital (SOMO) as presented in Figure 5f and 5g for **2a** and **2b**, respectively. The electron density clearly dictates the metal or ligand centric electron responsible for the respective EPR signature. The final appearance of metal-centered EPR with **2b** results in the presumption that the unpaired electron initially resides on the dithiolene ligand that later moves to the metal center to gain enhanced stability. Such a flow of electron from the molybdenum center to the ligand is observed only in the case of **2b**. The transient EPR signal of the radical species is uniquely observed in the frozen solution of partially oxidized **2b**. Other complexes in the series **2a–6b** on partial oxidation are not capable of displaying such transient species but directly show Mo(V)-centered EPR. This could be related to the inherent stability of the radical species in the case of **2b** which transiently appeared and quickly disappeared, generating the Mo(V) EPR signal. There is a variation in the diimine bite angle and dihedral angle of the thiolate residue (O–Mo–S–Ph) (Supporting Information Table S5) throughout the series of complexes **2a–6b**. It is worth noting that both the diimine bite angle and the thiolato dihedral angle of **2b** are the largest in the series (N–Mo–N = 71.15° and O–Mo–S–C = 105.0°). We presume that such a unique combination helps the one-electron oxidation centered on dithiolene in **2b** to gain enough stability to be observed as transient EPR species. Such a combination of the aforesaid metric parameters has not been observed for any other complex in the series. Computational studies on changing the diimine bite angle and the thiolato dihedral angle support such explanation (vide infra). EPR spectra of other pairs of complexes have been appended in Supporting Information Figure S4. Our results thus show that the radical species on dithiolene is of transient existence. Several unsaturated dithiolene complexes of transition metals having bis and tris dithiolene ligation are reported to be of noninnocent nature showing radical behavior.<sup>38,39</sup> Spin quantitation of the Mo(V) signal has been carried out using BDPA radical as the integration standard. Double integration provides  $0.8 \pm 0.05$  spins per molecule for both **2a** and **2b** (i.e., approximately 1 spin per monomeric molybdenum species).

The role of Moco in electron transfer remained unknown, but the function of pterindithiolene as the redox gate in the reactivation of the molybdenum center has been suggested for molybdenum enzymes.<sup>40</sup> Pterindithiolene can be visualized as the initial oxidant or reductant in the reactivation of the molybdenum center.<sup>41,42</sup> Thus, the formal oxidation state of molybdenum in the complex does not necessarily reflect the electronic picture of the complex. The oxidation state of the metal in relation to that of the complex as compared to complexes with unambiguous oxidation state has been determined from metal K-edge XAS studies.<sup>43</sup> It can be surmised from the EPR studies that the dithiolene ligand of the one-electron-oxidized species of **2b** is best described as a cation radical and thus emphasizes the pronounced noninnocent character of the dithiolene. The detailed study of such behavior is shown from DFT calculations (see computational results).

Photoelectron spectroscopic (PES) studies have supported the idea of dithiolene acting as an electronic buffer to the metal center.<sup>44</sup> It can be presumed that the apparent noninnocent behavior of pterindithiolene in the enzymes may reflect considerable protein–cofactor interactions, including the influence of amino acid coordination to molybdenum.

**Electrochemistry.** Consecutive reversible Mo(V)/Mo(IV) and Mo(VI)/Mo(V) redox couples are observed around 0.2 and 0.47 V (vs Ag/AgCl) for **2a** and **2b**, respectively (Figure 6a

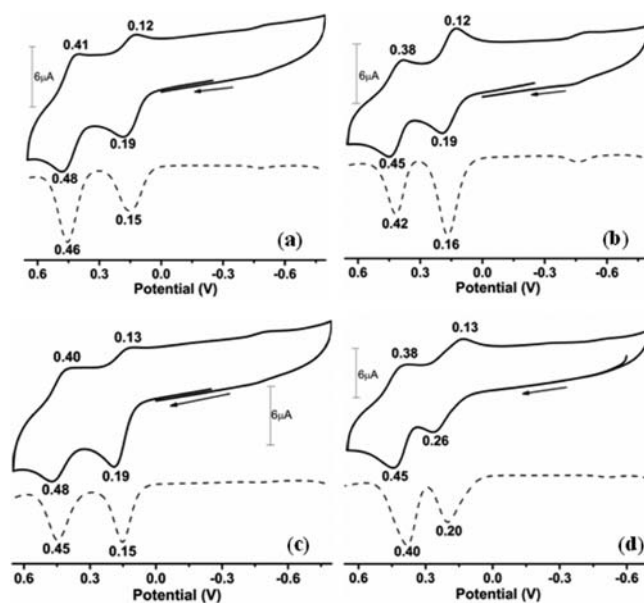


**Figure 6.** Cyclic voltammetric traces (scan rate 100 mV/s) and differential pulse polarograms (scan rate 20 mV/s, pulse width 50 ms, pulse period 200 ms, pulse amplitude 50 mV) of (a) **2a**, (b) **2b**, (c) **4a**, and (d) **6a** in dichloromethane.

and 6b). The reversible nature of these voltammograms indicates that the compounds are stable under electrochemical time scale and negligible structural deformation occurs on electrochemical oxidation, i.e., in the course of the electron transfer reaction. The reversible nature of the voltammograms was ascertained by the linear increase in peak currents (cathodic and anodic) with the increase in scan rate (Supporting Information Figure S5) and by observing the ratio between  $I_{pc}/I_{pa}$  which is close to unity.  $\Delta E$  values ranging from 60 to 80 mV also support the reversibility of these one electron transfer reactions. This has been substantiated by our electronic structure calculations for the Mo(IV), Mo(V), and Mo(VI) states retaining the crystallographically obtained structure with very little structural change. A recent report on a set of molybdenum complexes also validates this aspect.<sup>45</sup> It may be noted that the original shape of the voltammograms was retained after successive cycles, indicating high reproducibility of the electrode reactions. The two sequential one-electron oxidation steps could be associated with oxidation of the molybdenum centers from Mo(IV) to Mo(V) and from Mo(V) to Mo(VI). Our systems do not respond to any reduction step, contrary to the earlier report by Spence and co-workers.<sup>46</sup>

In *p*-NO<sub>2</sub> thiolate-substituted complexes **6a** and **6b** (Figure 6d for **6a**), the first oxidative response is quasireversible. However, the second oxidative response is reversible in these complexes. As expected, a slight increase in oxidation potential

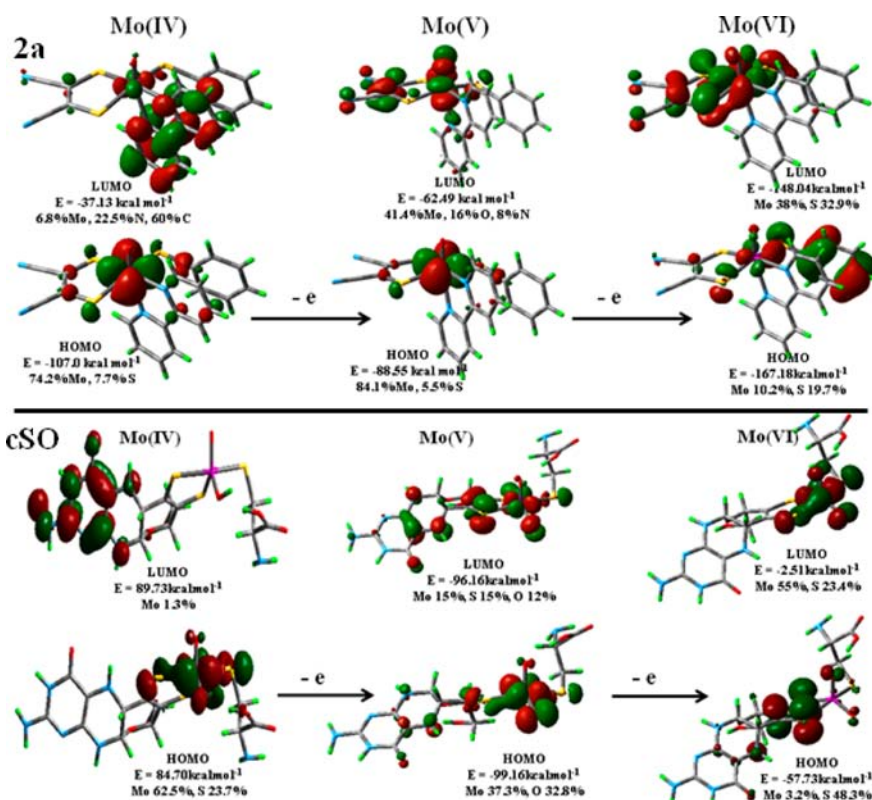


**Figure 7.** Comparison between the frontier orbitals of **2a** and native cSO active site. One-electron- and two-electron-oxidized species of **2a** are also depicted along with those of the Moco of cSO (isosurface cutoff value 0.04).

is also observed in these complexes from 0.19 to 0.26 V (first oxidation) as the remote substituent becomes electron withdrawing. Decreased electron density over the molybdenum center in **6a** and **6b** can be the possible reason for its reluctance to undergo oxidation.<sup>47</sup> Electrochemical oxidation removes electrons from the HOMO of the complexes. The modest susceptibility of the electrochemical process (Table S6 Supporting Information) on the  $-\text{SR}$  group indicates that some perturbation to the energy level is being caused by the remote substituent, at least in the case of the first oxidative process. A similar result was observed in  $[(\text{tp}^*)\text{MoO}(p\text{-OC}_6\text{H}_4\text{-Y})\text{Cl}]$  and  $[(\text{tp}^*)\text{MoO}(p\text{-SC}_6\text{H}_4\text{-Y})(\text{OPR}_3)]$ .<sup>47</sup> The linear dependence of the peak currents with the square root of the scan rate and a reverse-to-forward peak current ratio close to unity indicate a diffusion-controlled process. The peak-to-peak separation ( $\Delta E_p$ ) values suggest a typical one-electron redox process (Table S6 Supporting Information). For xanthine oxidase and sulfite oxidase, the redox potentials of the Mo centers differ by nearly 0.4 and 0.2 V for Mo(VI) to Mo(V) and Mo(V) to Mo(IV) states, respectively.<sup>48</sup> In the synthesized monomeric complexes, two oxidation potentials differ by  $\sim 0.25$  V.

**Computational Analysis.** Ground-state DFT calculations were performed to interpret the experimental electrochemical results in light of the redox processes involved.<sup>51</sup> The starting geometries were taken from the respective X-ray crystal structures. We used the B3LYP and BP86 functionals, which are commonly used to describe the electronic structure in  $M(\text{diimine})(\text{dithiolene})$ <sup>32</sup> and other biologically relevant complexes.<sup>55</sup> Geometry optimization of the structures of the oxidized states of the synthesized complexes were carried out using both the functionals, but single-point calculations

reported were obtained using B3LYP.<sup>34d</sup> The electronic structure of hexacoordinated complexes is described in terms of the observed d-orbital splitting pattern originally propounded by Jørgensen and Gray et al. in explaining the bonding in molybdenyl and vanadyl complexes.<sup>52</sup> Noninnocent dithiolene<sup>53</sup> and the  $\pi$  orbital of diimine cause a large HOMO–LUMO gap in  $\{\text{OMo(IV)}(\text{diimine})(\text{dithiolene})\}$  complexes (Figure 7, top panel, left). The terminal oxo group attached to Mo is an extremely potent  $\sigma$  and  $\pi$  donor.  $d_{z^2}$  and  $d_{x^2-y^2}$  are destabilized by the  $\sigma$ - and  $\pi$ -antibonding interaction with such terminal oxo group.<sup>52b,c</sup> Due to strong axial compression of the oxo ligand, the  $d_{xy}$  orbital is further stabilized as compared to the  $d_{xz}$  and  $d_{yz}$  orbitals.  $d_{xy}$  remains principally nonbonding, resulting in a  $d_{xy}^2$  electronic configuration in the ground state for Mo(IV). The lowest energy electronic transition is therefore expected to be metal centered.

In accordance to the expected electronic population, the HOMO is found to be principally metal centered ( $d_{xy}$  orbital of Mo) in **2a–6b**. Calculations indicate that the ligand frontier orbital electron density is largely localized on the sulfur atoms of the dithiolate and the thiolate moiety (HOMO-1), which is energetically lower than the metal-centered HOMO. Charge-deficient dithiolates like  $\text{mnt}^{2-}$  are harder to oxidize than others having alkyl or aryl substitution. This also supports the fact that no ligand-centered oxidation based on  $\text{mnt}^{2-}$  is observed in the potential window used experimentally. The LUMO is based on the  $\pi^*$  orbital of diimine (top panel, Figure 7). This supports the MLCT band observed experimentally. This type of LUMO is common for  $M(\text{diimine})(\text{dithiolene})$  systems.<sup>32</sup> The HOMO of the molybdenum active site in cSO is also based on the metal center (Figure 7, bottom panel). The one-electron-oxidized species of **2a** showed a metal-based HOMO which corroborates

the observed EPR signal characteristic of the Mo(V) center. The LUMO in this case also has considerable metal contribution (Figure 7, top panel, middle column). The fully oxidized Mo(VI) center however depicts a ligand-centered HOMO and metal-based LUMO (Figure 7, top panel, right-hand column) similar to that observed for the native active site (Figure 7, bottom panel, right-hand column)

In addition to the effects of the first coordination sphere on the electronic environment around the metal center, the second coordination sphere also has some influence on the covalence of metal–ligand bonds.<sup>54</sup> Sulfur K-edge XAS studies primarily used to identify these subtle changes deciphered the non-innocence of dithiolene among other factors, causing changes in the formal oxidation state of the metal.<sup>54</sup> Apparent noninnocent behavior of the Moco in most enzymes may reflect significant protein–cofactor interactions, including the influence of amino acid coordination to the metal center. Several groups have used bulky nitrogenous ligand in designing respective model complexes to proxy the protein coordination to the Moco.<sup>9,31d,e</sup> However, no rationalization on the effects of such binding to the metal center has been proposed from a computational point of view. We strived to pinpoint that a subtle change in such binding can lead to a differently populated frontier orbital which can explain the function of dithiolene as the electron transfer gateway. This provides a plausible pathway for electron transfer regeneration of the Mo center in pterindithiolene-containing enzymes.

Dithiolenes have been proposed to couple with the metal center into efficient superexchange pathways to facilitate regeneration of the enzyme by electron transfer. The electronic buffering effect of equatorial dithiolene against the severe perturbation of metal-centered HOMO has been observed by PES study of hydrotrispyrazolyl borate complexes.<sup>44</sup> In molybdenum enzymes, a variety of possible roles for the pterindithiolene can be envisaged including modulation of the redox potential and as an electron transfer gateway to other redox partners.<sup>55</sup> Evidence from the reactivity can be cited for direct involvement of pyranopterindithiolene in electron transfer.<sup>55</sup>

On stepwise changing the bite angle of the diimine and the dihedral angle of the thiolate ligand the coupled effect can lead to a difference in the electronic population typically represented in the case of **2a** and **2b**. A schematic diagram has been presented in Figure 8.

The bite angle of diimine and dihedral angle of the thiolate ligand in **2a** has been changed stepwise to those of **2b**, i.e., the

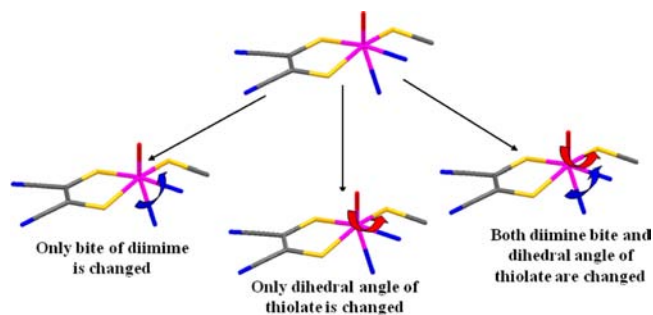


**Figure 8.** Illustration of the systematic modification of diimine bite angle and thiolate torsional angle leading to a ligand-centered HOMO from a metal-centered HOMO and vice versa on one-electron oxidation of **2a** and **2b**.

diimine bite was changed from  $70.0^\circ$  to  $71.1^\circ$  and the dihedral angle of the thiolate ligand was changed from  $99.6^\circ$  to  $105.5^\circ$ . Similar treatment has been carried out for **2b** replacing its bite angle of  $71.1^\circ$  to  $70.0^\circ$  and dihedral angle of  $105.5^\circ$  to  $99.6^\circ$ . It was observed that in the course of this stepwise treatment the metal-based SOMO in **2a** (Figure 9A, extreme left) is being converted to a ligand-based SOMO (Figure 9A, extreme right), dithiolene being the principle contributor to the SOMO. As anticipated, such a modification effected in **2b** enhances the metal contribution considerably to the SOMO (Figure 9B, extreme right column). The untreated SOMO for **2b** was entirely delocalized on the dithiolene ligand with contributions also from the thiolate sulfur (Figure 9B, extreme left). Thus, it can be observed that a subtle change in the bite angle of diimine which is being used as a place holder for surrounding bulky protein in the native enzyme and dihedral angle of the thiolate ligand brings about a change in the electronic population of the SOMO in the Mo(V) state of **2a** and **2b**.

The transient existence of a delocalized ligand-centered EPR observed in **2b** can thus be corroborated by the ligand-based SOMO. It can be further observed that the energies of the SOMOs of **2a** and **2b** are comparable, though the dithiolene-based SOMO is slightly destabilized as compared to the metal-based SOMO. This supports the ability of the dithiolene ligand to undergo oxidation at redox potentials comparable to that of the metal center. Such observation is consistent with the electronic structure of the metal–dithiolene system involving extensive delocalization and at least partial ligand participation in redox processes. Dithiolate folding has provided a mechanism which could rationalize the “electronic buffering” by these ligands in terms of the overlap between the in-plane metal orbitals to the other redox partners via pyranopterin.<sup>56</sup> The effect of the diimine bite could help us to envisage the role of the bulky protein in modulating the electron transfer phenomena to the adjacent domain of cytochromes in SO. The function of the coordinating thiolate moiety in modulating the properties of transition metal complexes is also of considerable interest. Variation of the thiolate ligand with the substituent in the para position controls the reduction potential of the molybdenum center to influence the stability of the Mo(V) state as observed from electrochemical studies. Such stability order has already been shown by X-ray absorption spectroscopy and DFT calculations on a series of Mo(VI) complexes.<sup>57</sup>

## CONCLUSION

The work described here provides a detailed study on some synthetic analogue systems of the reduced molybdenum center of enzymes belonging to the sulfite oxidase family and their participation in electron transfer reaction akin to the molybdenum active site. These complexes possess an equatorial thiolate ligation and a dithiolene moiety closely simulating the cysteinyl residue in the native system. The fifth and sixth coordination sites around molybdenum are blocked by aromatic diimines to prevent dimerization on oxidation. The analogue systems have been shown to participate in electron transfer via a pentavalent EPR-active species similar to the native enzyme with minimum structural deformation, as depicted by two reversible oxidative responses. In one of the analogous systems, a transient dithiolene-based EPR signal is observed, supporting the role of pterin–dithiolene as an electron transfer gate in the catalytic cycle of molybdoenzymes. A stepwise rationale has been provided from the electronic structure calculations in explaining this subtle change in

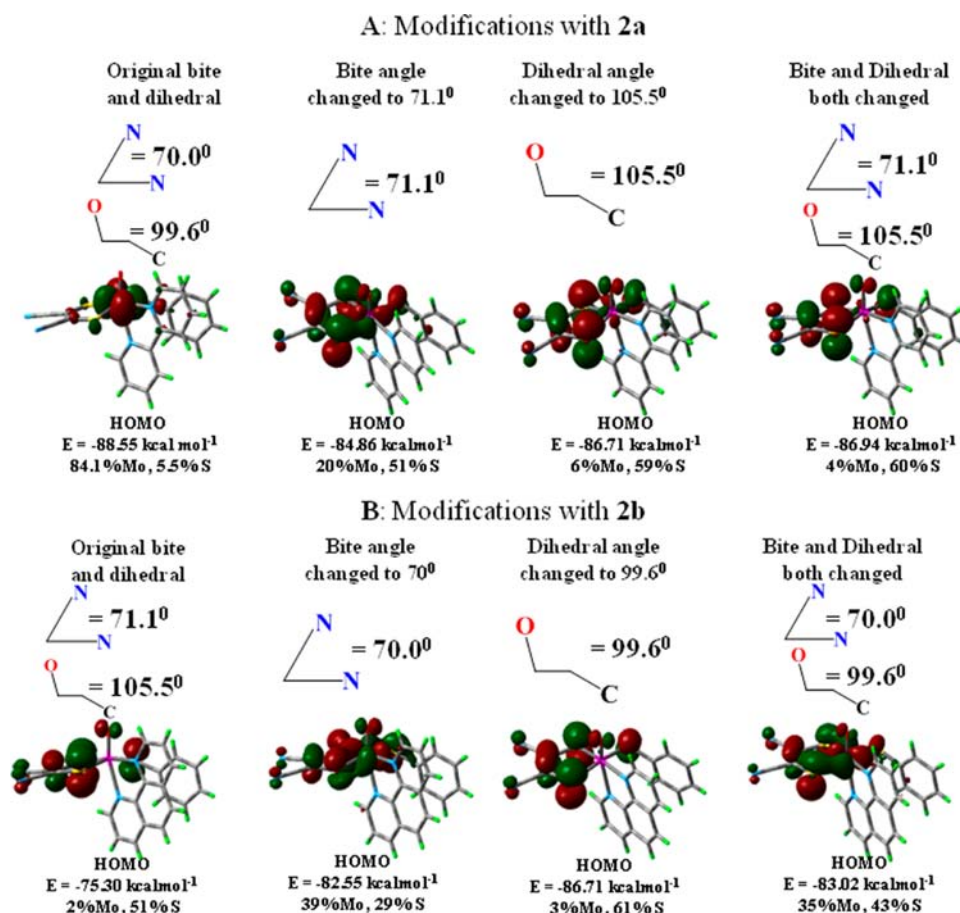


**Figure 9.** Systematic modification of diimine bite angle and thiolato torsion angle leading to a ligand-centered HOMO from a metal-centered HOMO and vice versa on one-electron oxidation of **2a** and **2b** (isosurface cutoff value 0.04).

electronic behavior. DFT calculations depict the similarity between the reduced, semireduced, and fully oxidized (resting state) forms of the native molybdenum center with the synthesized complexes and their one-electron and fully oxidized counterparts.

## ■ ASSOCIATED CONTENT

### ● Supporting Information

X-ray crystallographic data in CIF format, relevant crystallographic parameters, bond length and bond angle data along with an overlay of the molybdenum active site of the SO family enzymes with synthesized complexes, room-temperature and frozen solution EPR spectra, cyclic voltammetric data, and frontier orbital calculations. This material is available free of charge via the Internet at <http://pubs.acs.org>.

## ■ AUTHOR INFORMATION

### Corresponding Author

\*E-mail: [abya@iitk.ac.in](mailto:abya@iitk.ac.in), [protozyme@gmail.com](mailto:protozyme@gmail.com).

### Notes

The authors declare no competing financial interest.

## ■ ACKNOWLEDGMENTS

S.S. thanks the DST, New Delhi. for generous funding under the special initiative bioinorganic project, and J.M. thanks CSIR, India, for a Senior Research Fellowship.

## ■ REFERENCES

- (1) (a) McLeod, R. M.; Farkas, W.; Fridovich, I.; Handler, P. *J. Biol. Chem.* **1961**, *236*, 1841. (b) In *Molybdenum Enzymes*; Spiro, T. G., Ed.; John Wiley and Sons: New York, 1985.
- (2) Hille, R. *Chem. Rev.* **1996**, *96*, 2757.
- (3) (a) Loschi, L.; Brokx, S. J.; Hills, T. L.; Zhang, G.; Bertero, M. G.; Lovering, A. L.; Weiner, J. H.; Strynadka, N. C. *J. Biol. Chem.* **2004**, *279*, 50391. (b) Havelius, K. G. V.; Reschke, S.; Horn, S.; Doring, A.; Niks, D.; Hille, R.; Schulzke, C.; Leimkuhler, S.; Haumann, M. *Inorg. Chem.* **2011**, *50*, 741.
- (4) Kisker, C.; Schindelin, H.; Pacheco, A.; Wehbi, W. A.; Garrett, R. M.; Rajagopalan, K. V.; Enemark, J. H.; Rees, D. C. *Cell* **1997**, *91*, 973.
- (5) (a) Ueyama, N.; Oku, H.; Kondo, M.; Okamura, T.; Yoshinaya, N.; Nakamura, A. *Inorg. Chem.* **1996**, *35*, 643. (b) Lorber, C.; Plutino, M. R.; Elding, L. I.; Nordlander, E. *J. Chem. Soc., Dalton Trans.* **1997**, 3997. (c) Tucci, G. C.; Donahue, J. P.; Holm, R. H. *Inorg. Chem.* **1998**, *37*, 1602. (d) Das, S. K.; Chaudhury, P. K.; Biswas, D.; Sarkar, S. *J. Am. Chem. Soc.* **1994**, *116*, 9061.
- (6) (a) Lim, B. S.; Willer, M. W.; Miao, M.; Holm, R. H. *J. Am. Chem. Soc.* **2001**, *123*, 8343. (b) Jalilvand, F.; Lim, B. S.; Holm, R. H.; Hedman, B.; Hodgson, K. O. *Inorg. Chem.* **2003**, *42*, 5531.
- (7) (a) Dhawan, I.; Enemark, J. H. *Inorg. Chem.* **1996**, *35*, 4873. (b) Peariso, K.; Chohan, B. S.; Carrano, C. J.; Kirk, M. L. *Inorg. Chem.* **2003**, *42*, 6194. (c) Mader, M. L.; Carducci, M. D.; Enemark, J. H. *Inorg. Chem.* **2000**, *39*, 525. (d) Dhawan, I. K.; Pacheco, A.; Enemark, J. H. *J. Am. Chem. Soc.* **1994**, *116*, 7911.
- (8) (a) Nicholas, K. M.; Khan, M. A. *Inorg. Chem.* **1987**, *26*, 1633. (b) Sugimoto, H.; Siren, K.; Tsukube, H.; Tanaka, K. *Eur. J. Inorg. Chem.* **2003**, 2633.

- (9) (a) Xiao, Z.; Young, C. G.; Enemark, J. H.; Wedd, C. G. *J. Am. Chem. Soc.* **1992**, *114*, 9194. (b) Xiao, Z.; Bruck, M. A.; Enemark, J. H.; Young, C. G.; Wedd, A. G. *Inorg. Chem.* **1996**, *35*, 7508.
- (10) Majumdar, A.; Sarkar, S. *Coord. Chem. Rev.* **2011**, *255*, 1039.
- (11) (a) King, R. B. *Inorg. Chem.* **1963**, *2*, 641. (b) McCleverty, J. A.; Locke, J.; Wharton, E. J.; Gerloch, M. *J. Chem. Soc. A* **1968**, 816. (c) Boyde, S.; Garner, C. D.; Enemark, J. H.; Bruck, M. A.; Kristofzski, J. G. *J. Chem. Soc., Dalton Trans.* **1987**, 2267. (d) Kapre, R. R.; Bothe, E.; Weyhermüller, T.; DeBeer George, S.; Wieghardt, K. *Inorg. Chem.* **2007**, *46*, 5642.
- (12) Pal, K.; Maiti, R.; Chaudhury, P. K.; Sarkar, S. *Inorg. Chim. Acta* **2007**, *360*, 2721.
- (13) SAINT, version 5.6; Bruker AXS Inc.: Madison, WI, 2000.
- (14) Altomare, A.; Burla, M. C.; Camalli, M.; Cascarano, G. L.; Giacovazzo, C.; Guagliardi, A.; Moliterni, A. G. G.; Polidori, G.; Spagna, R. *J. Appl. Crystallogr.* **1999**, *32*, 115.
- (15) Sheldrick, G. M. *SHELX97. Programs for Crystal Structure Analysis (Release 97-2)*; University of Gottingen: Gottingen, Germany, 1997.
- (16) Farrugia, L. J. *J. Appl. Crystallogr.* **1997**, *30*, 565.
- (17) Frisch, M. J.; Trucks, G. W.; Schlegel, H. B.; Scuseria, G. E.; Robb, M. A.; Cheeseman, J. R.; Montgomery, Jr., J. A.; Vreven, T.; Kudin, K. N.; Burant, J. C.; Millam, J. M.; Iyengar, S. S.; Tomasi, J.; Barone, V.; Mennucci, B.; Cossi, M.; Scalmani, G.; Rega, N.; Petersson, G. A.; Nakatsuji, H.; Hada, M.; Ehara, M.; Toyota, K.; Fukuda, R.; Hasegawa, J.; Ishida, M.; Nakajima, T.; Honda, Y.; Kitao, O.; Nakai, H.; Klene, M.; Li, X.; Knox, J. E.; Hratchian, H. P.; Cross, J. B.; Bakken, V.; Adamo, C.; Jaramillo, J.; Gomperts, R.; Stratmann, R. E.; Yazyev, O.; Austin, A. J.; Cammi, R.; Pomelli, C.; Ochterski, J. W.; Ayala, P. Y.; Morokuma, K.; Voth, G. A.; Salvador, P.; Dannenberg, J. J.; Zakrzewski, V. G.; Dapprich, S.; Daniels, A. D.; Strain, M. C.; Farkas, O.; Malick, D. K.; Rabuck, A. D.; Raghavachari, K.; Foresman, J. B.; Ortiz, J. V.; Cui, Q.; Baboul, A. G.; Clifford, S.; Cioslowski, J.; Stefanov, B. B.; Liu, G.; Liashenko, A.; Piskorz, P.; Komaromi, I.; Martin, R. L.; Fox, D. J.; Keith, T.; Al-Laham, M. A.; Peng, C. Y.; Nanayakkara, A.; Challacombe, M.; Gill, P. M. W.; Johnson, B.; Chen, W.; Wong, M. W.; Gonzalez, C.; Pople, J. A. *Gaussian 03 (Revision B.04)*; Gaussian, Inc.: Pittsburgh, PA, 2003.
- (18) (a) Becke, A. D. *J. Chem. Phys.* **1993**, *98*, 5648. (b) Lee, C.; Yang, W.; Parr, R. G. *Phys. Rev. B* **1988**, *37*, 785.
- (19) (a) Becke, A. D. *Phys. Rev. A* **1988**, *38*, 3098. (b) Perdew, J. P. *Phys. Rev. B* **1986**, *33*, 8822.
- (20) Paterson, G. A.; Al-Laham, M. A. *J. Chem. Phys.* **1991**, *94*, 6081.
- (21) (a) Hay, P. J.; Wadt, W. R. *J. Chem. Phys.* **1985**, *82*, 270. (b) Wadt, W. R.; Hay, P. J. *J. Chem. Phys.* **1985**, *82*, 284.
- (22) Eckert, F.; Klamt, A. *AICHE J.* **2002**, *48*, 369.
- (23) (a) Gorelsky, S. I. *AOMix: Program for Molecular Orbital Analysis*; University of Ottawa: Ottawa, 2007; <http://www.sg-chem.net/>. (b) Gorelsky, S. I.; Lever, A. B. P. *J. Organomet. Chem.* **2001**, *635*, 187.
- (24) Mitra, J.; Sarkar, S. *Ind. J. Chem., Sect A* **2011**, *50A*, 401.
- (25) Blake, A. B.; Cotton, F. A.; Wood, J. S. *J. Am. Chem. Soc.* **1964**, *86*, 3024.
- (26) Saha, H. K.; Banerjee, A. K. *J. Inorg. Nucl. Chem.* **1972**, *34*, 1861.
- (27) Maria, P. D.; Fini, A.; Hall, F. M. *J. Chem. Soc., Perkin Trans. 2* **1977**, 149.
- (28) Nagarajan, K.; Joshi, H. K.; Chaudhuri, P. K.; Pal, K.; Cooney, J. A.; Enemark, J. H.; Sarkar, S. *Inorg. Chem.* **2004**, *43*, 4532.
- (29) (a) Bahr, G.; Schleitzer, B. *Chem. Ber.* **1955**, *88*, 1771. (b) Bahr, G. *Angew. Chem.* **1956**, *68*, 525. (c) Stiefel, E. I.; Bennet, L. E.; Dori, Z.; Crawford, T. H.; Simo, C.; Gray, H. B. *Inorg. Chem.* **1970**, *9*, 281. (d) Davidson, A.; Holm, R. H. *Inorg. Synth.* **1967**, *10*, 8.
- (30) Scarborough, C. C.; Wieghardt, K. *Inorg. Chem.* **2011**, *50*, 9773.
- (31) (a) Rana, A.; Dinda, R.; Ghosh, S.; Blake, A. J. *Polyhedron* **2003**, *22*, 3075. (b) Craig, J. A.; Horlan, E. W.; Synder, B. S.; Whitener, M. A.; Holm, R. H. *Inorg. Chem.* **1989**, *28*, 2082. (c) Senger, R. S.; Nemykin, V. N.; Basu, P. *J. Inorg. Biochem.* **2008**, *102*, 748. (d) Roberts, S. A.; Young, C. G.; Cleland, W. E., Jr.; Ortega, R. B.; Enemark, J. H. *Inorg. Chem.* **1988**, *27*, 3044. (e) Young, C. G.; Roberts, S. A.; Ortega, R. B.; Enemark, J. H. *J. Am. Chem. Soc.* **1987**, *109*, 2938.
- (32) Mitsopoulou, C. A. *Coord. Chem. Rev.* **2010**, *254*, 1448.
- (33) (a) Vlcek, A., Jr.; Zális, S. *Coord. Chem. Rev.* **2007**, *251*, 258. (b) Buhl, M.; Reimann, C.; Pantazis, D. A.; Bredow, T.; Neese, F. *J. Chem. Theory Comput.* **2008**, *4*, 1449.
- (34) (a) Daku, L. M. L.; Vargus, A.; Hauser, A.; Fouqueau, A.; Casida, M. E. *Chem. Phys. Chem.* **2005**, *6*, 1393. (b) Reiher, M.; Salomon, O.; Hess, B. A. *Theor. Chem. Acc.* **2001**, *107*, 48. (c) Ye, S.; Neese, F. *Inorg. Chem.* **2010**, *49*, 772. (d) Surawatanawong, P.; Sproules, S.; Neese, F.; Wieghardt, K. *Inorg. Chem.* **2011**, *50*, 12064.
- (35) Dey, A. *J. Am. Chem. Soc.* **2010**, *132*, 13892.
- (36) (a) Joshi, H. K.; Cooney, J. A.; Inscore, F. E.; Gruhn, N. E.; Lichtenberger, D. L.; Enemark, J. H. *Proc. Natl. Acad. Sci. U.S.A.* **2003**, *100*, 3719. (b) Lauher, J. W.; Hoffmann, R. *J. Am. Chem. Soc.* **1976**, *98*, 1729.
- (37) Cohen, H. J.; Fridovich, I.; Rajagopalan, K. V. *J. Biol. Chem.* **1971**, *246*, 367.
- (38) (a) Davison, A.; Edelstein, N.; Holm, R. H.; Maki, A. H. *J. Am. Chem. Soc.* **1964**, *86*, 2799. (b) Davison, A.; Edelstein, N.; Holm, R. H.; Maki, A. H. *J. Am. Chem. Soc.* **1963**, *85*, 3049. (c) Sproules, S.; Banerjee, P.; Weyhermüller, T.; Yan, Y.; Donahue, J. P.; Wieghardt, K. *Inorg. Chem.* **2011**, *50*, 7106.
- (39) Begum, A.; Moula, G.; Sarkar, S. *Chem.—Eur. J.* **2010**, 12324.
- (40) Burgmayer, S. J. N. *Struct. Bonding (Berlin)* **1998**, *92*, 67.
- (41) (a) Tenderholt, A. L.; Szilagy, R. K.; Holm, R. H.; Hodgson, K. O.; Hedman, B.; Solomon, E. I. *Inorg. Chem.* **2008**, *47*, 6382. (b) Sarangi, R.; DeBeer George, S.; Rudd, D. J.; Szilagy, R. K.; Ribas, X.; Rovira, C.; Almeida, M.; Hodgson, K. O.; Hedman, B.; Solomon, E. I. *J. Am. Chem. Soc.* **2007**, *129*, 2316.
- (42) Szilagy, R. K.; Lim, B. S.; Glaser, T.; Holm, R. H.; Hedman, B.; Hodgson, K. O.; Solomon, E. I. *J. Am. Chem. Soc.* **2003**, *125*, 9158.
- (43) (a) Banerjee, P.; Sproules, S.; Weyhermüller, T.; DeBeer George, S.; Wieghardt, K. *Inorg. Chem.* **2009**, *48*, 5829. (b) Kapre, R.; Ray, K.; Sylvestre, I.; Weyhermüller, T.; DeBeer George, S.; Neese, F.; Wieghardt, K. *Inorg. Chem.* **2006**, *45*, 3499. (c) Ray, K.; DeBeer George, S.; Solomon, E. I.; Wieghardt, K.; Neese, F. *Eur. J. Inorg. Chem.* **2007**, *13*, 2783. (d) Milsmann, C.; Bill, E.; Weyhermüller, T.; DeBeer George, S.; Wieghardt, K. *Inorg. Chem.* **2009**, *48*, 9754. (e) Sproules, S.; Weyhermüller, T.; DeBeer, S.; Wieghardt, K. *Inorg. Chem.* **2010**, *49*, 5241.
- (44) Westcott, B. L.; Gruhn, N. E.; Enemark, J. H. *J. Am. Chem. Soc.* **1998**, *120*, 3382.
- (45) Huttinger, K.; Forster, C.; Bund, T.; Hinderberger, D.; Heinze, K. *Inorg. Chem.* **2012**, *51*, 4180.
- (46) Boyd, I. W.; Spence, J. T. *Inorg. Chem.* **1982**, *21*, 1602.
- (47) (a) Graff, J. N.; McElhaney, A. E.; Basu, P.; Gruhn, N. E.; Chang, C.-S. J.; Enemark, J. H. *Inorg. Chem.* **2002**, *41*, 2642. (b) Basu, P.; Nemykin, V. N.; Sengar, R. S. *Inorg. Chem.* **2009**, *48*, 6303.
- (48) Solomonson, L. P.; Barber, M. J.; Howard, W. D.; Johnson, J. L.; Rajagopalan, K. V. *J. Biol. Chem.* **1984**, *259*, 849.
- (49) Cohen, H. J.; Fridovich, I. *J. Biol. Chem.* **1971**, *246*, 359.
- (50) (a) Sugio, T.; Katagiri, Y.; Moriyama, M.; Zhèn, Y. L.; Inagaki, K.; Tano, T. *Appl. Environ. Microbiol.* **1988**, *54*, 153. (b) de Gong, G. A. H.; Yang, J. A.; Bos, P.; deVries, S.; Keunen, J. G. *J. Mol. Catal. B* **2000**, *8*, 61.
- (51) (a) Johnson, J. L.; Rajagopalan, K. V. *J. Biol. Chem.* **1977**, 252, 2017. (b) Pushie, M. J.; George, G. N. *Coord. Chem. Rev.* **2011**, *255*, 1044.
- (52) (a) Jørgensen, C. K. *Acta Chem. Scand.* **1957**, *11*, 73. (b) Ballhausen, C. J.; Gray, H. B. *Inorg. Chem.* **1962**, *1*, 111. (c) Winkler, J. R.; Gray, H. B. *Comments Inorg. Chem.* **1981**, *1*, 257.
- (53) Eisenberg, R.; Gray, H. B. *Inorg. Chem.* **2011**, *50*, 9741.
- (54) Peariso, K.; Helton, M. E.; Duesler, E. N.; Shadle, S. E.; Kirk, M. L. *Inorg. Chem.* **2007**, *46*, 1259.
- (55) Rajagopalan, K. V. *Adv. Enzymol. Relat. Areas Mol. Biol.* **1991**, *64*, 215.

(56) Inscore, F. E.; McNaughton, R.; Westcott, B. L.; Helton, M. E.; Jones, R.; Dhawan, I. K.; Enemark, J. H.; Kirk, M. L. *Inorg. Chem.* **1999**, *38*, 1401.

(57) (a) Musie, G.; Reibenspies, J. H.; Darensbourg, M. Y. *Inorg. Chem.* **1998**, *37*, 302. (b) Izumi, Y.; Glaser, T.; Rose, K.; McMaster, J.; Basu, P.; Enemark, J. H.; Hedman, B.; Hodgson, K. O.; Solomon, E. I. *J. Am. Chem. Soc.* **1999**, *121*, 10035.

(58) CCDC 890840–890842 and CCDC 890845–890851 contain the supplementary crystallographic data for compounds **1–2b** and **3a–6b**. These data can be obtained free of charge from the Cambridge Crystallographic data Centre via [www.ccdc.cam.ac.uk/data\\_request/cif](http://www.ccdc.cam.ac.uk/data_request/cif).